AGU Advances

Supporting Information for

Runoff reconstructions and future projections indicate highly variable water supply from Pacific Rim water towers

Weipeng Yue [1,2,3], Max C.A. Torbenson [2], Feng Chen [1,3,4,5*], Frederick Reinig [2], Jan Esper [2,6*], Edurne Martinez del Castillo [2], Shijie Wang [1,3], Xiaoen Zhao [1,3,4], Mao Hu [1,3,4], Yang Xu [1], Martín A. Hadad [7], Álvaro González-Reyes [8], Fidel A. Roig [7,8], Tiyuan Hou [1,3], Honghua Cao [1,3,4], Hechuan Wang [1], Heli Zhang [1,5], Junqiang Niu [1], Youping Chen [1,3]

1 Yunnan Key Laboratory of International Rivers and Transboundary Eco-Security, Institute of International Rivers and Eco-Security, Yunnan University, Kunming, China

2 Department of Geography, Johannes Gutenberg University, Mainz, Germany

3 State Key Laboratory for Vegetation Structure, Function and Construction (VegLab), Yunnan University, Kunming, China

4 Southwest United Graduate School, Kunming, China

5 Key Laboratory of Tree-ring Physical and Chemical Research of the China Meteorological Administration/Xinjiang Laboratory of Tree-ring Ecology, Institute of Desert Meteorology, China Meteorological Administration, Urumqi, China

6 Global Change Research Institute (CzechGlobe), Czech Academy of Sciences, Brno, Czech Republic

7 Laboratorio de Dendrocronología de Zonas Áridas-Instituto y Museo de Ciencias Naturales, Universidad Nacional de San Juan, CIGEOBIO (CONICET-UNSJ), San Juan, Argentina

8 Instituto de Ciencias de la Tierra, Facultad de Ciencias, Universidad Austral de Chile, Valdivia, Chile

Corresponding author:

Feng Chen (feng653@163.com)

Jan Esper (esper@uni-mainz.de)

Contents of this file

Introduction

Supplementary figures and tables are cited in the main text and provide details regarding our methodology and other supporting information. All references can be found in the main text.

Figure S1. Display of some tree species and growth habitats in the Central China water tower (CCWT).

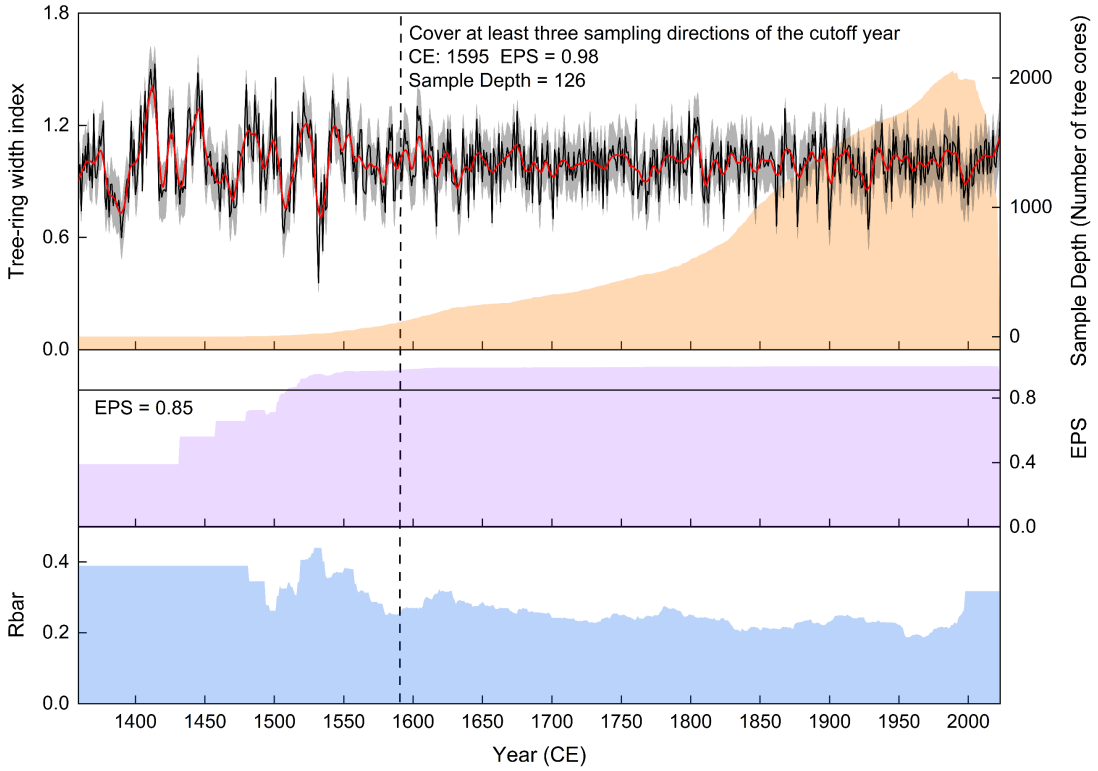

Figure S2. The composite chronology for the Central China water tower (CCWT) (thin black line), with decadal variability shown using an 11-year low-pass filter. The gray shaded area represents the ±1 standard deviation range, while the orange background indicates tree-ring sample depth. The purple background below shows the variation in the Expressed Population Signal (EPS), calculated using a 51-year window with a 50-year lag, with a reconstruction reliability threshold set at 0.85. The blue background represents the statistical data for the mean inter-series correlation (Rbar). The strict start year for the reconstruction was determined based on the first year when sampling coverage included growth in three directions, which is 1595 (See Table S1 for more details of the sampling sites). In that year, 126 cores were sampled, and the EPS value was 0.98.

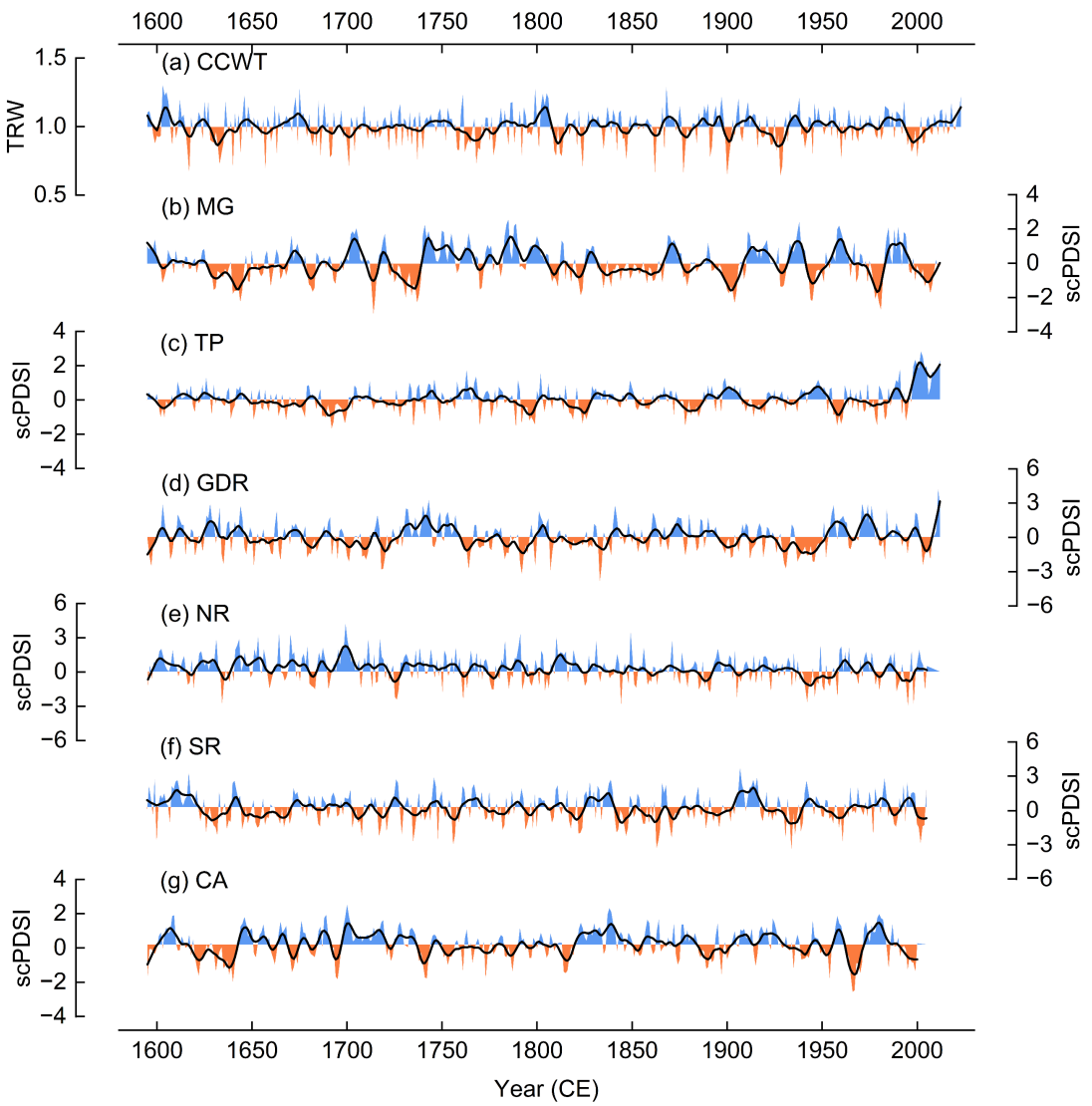

Figure S3. Proxy data for runoff depth reconstruction in the Pacific Rim water towers. The Central China water tower (CCWT) (a) is represented by tree-ring width data (TRW), while the others (b) to (g) are reconstructed from drought atlas data (scPDSI) based on tree-ring records, including the Mongolian Plateau (MG), Tibetan Plateau (TP), Great Dividing Range (GDR), Northern Rockies (NR), Southern Rockies (SR), and Central Andes (CA). All proxy data for the water towers are aligned to a uniform starting year. The thick black line represents the 11-year low-pass filtered results, and the shaded areas indicate the high and low value zones of the proxy data. For more details on proxy data, see Table S2.

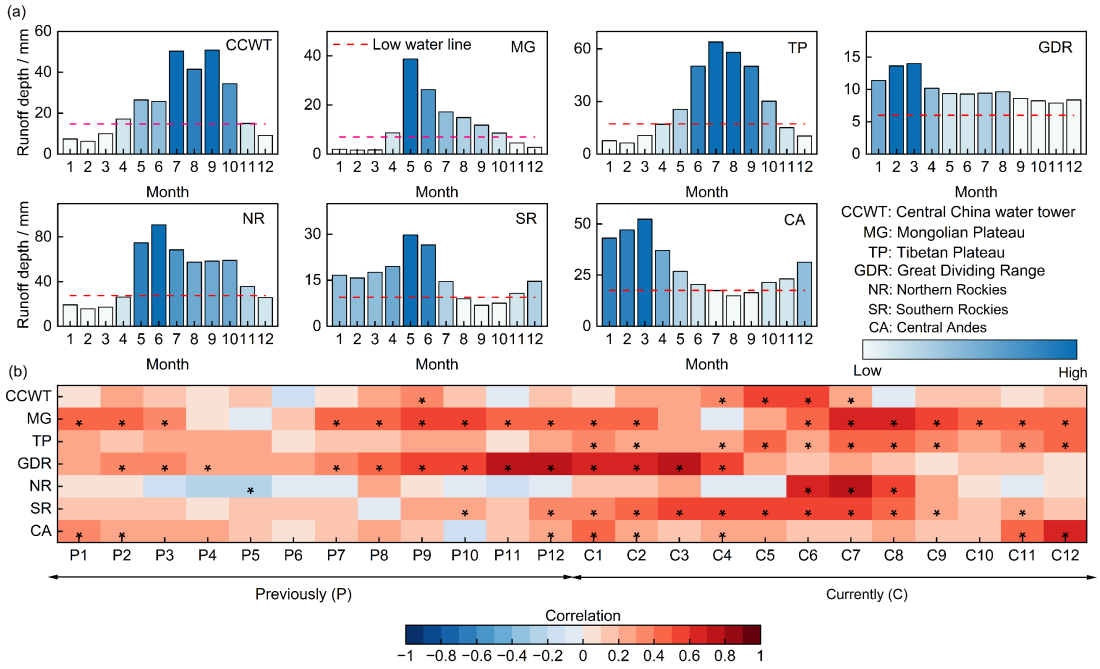

Figure S4. Hydrological data of runoff depth in the Pacific Rim water towers and its response relationship with proxy data. (a) The multi-year monthly distribution characteristics of hydrological runoff depth in the Pacific Rim water towers. The red dashed line represents the low-runoff threshold, with months over the dashed line indicating the flood season. Darker colors indicate higher surface runoff depth, while lighter colors indicate the opposite. (b) Correlation characteristics between proxy data of reconstructed runoff depth and hydrological data in the Pacific Rim water towers. Please note that when the monthly mean runoff depth accounts for less than 5% of the annual runoff depth, it enters the dry season. The red threshold line is calculated by reverse calculation based on this definition. P represents the previous year, C represents the current year, and "*" denotes significance at the 95% confidence level.

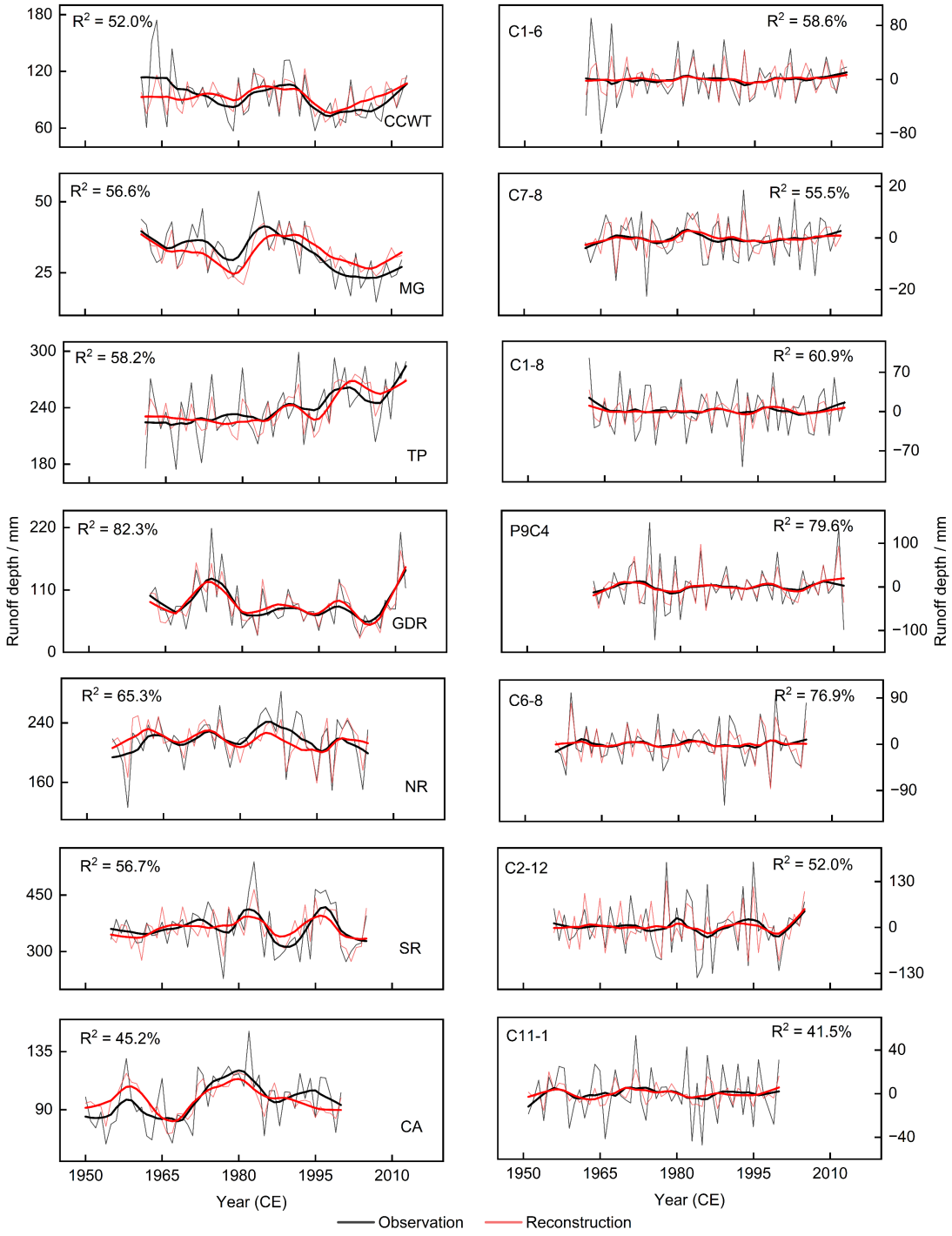

Figure S5. Comparison between reconstructed and observed runoff depth in the Pacific Rim water towers. The red line represents the reconstruction, and the black line represents observations. An 11-year window with the LOWESS method is applied for low-pass filtering to capture the decadal variability in reconstructed and observed runoff depth. The left panel shows the original comparison, while the right panel

displays the comparison after first-difference calculations. From top to bottom, they are the Central China water tower (CCWT), the Mongolian Plateau (MG), Tibetan Plateau (TP), Great Dividing Range (GDR), Northern Rockies (NR), Southern Rockies (SR), and Central Andes (CA).

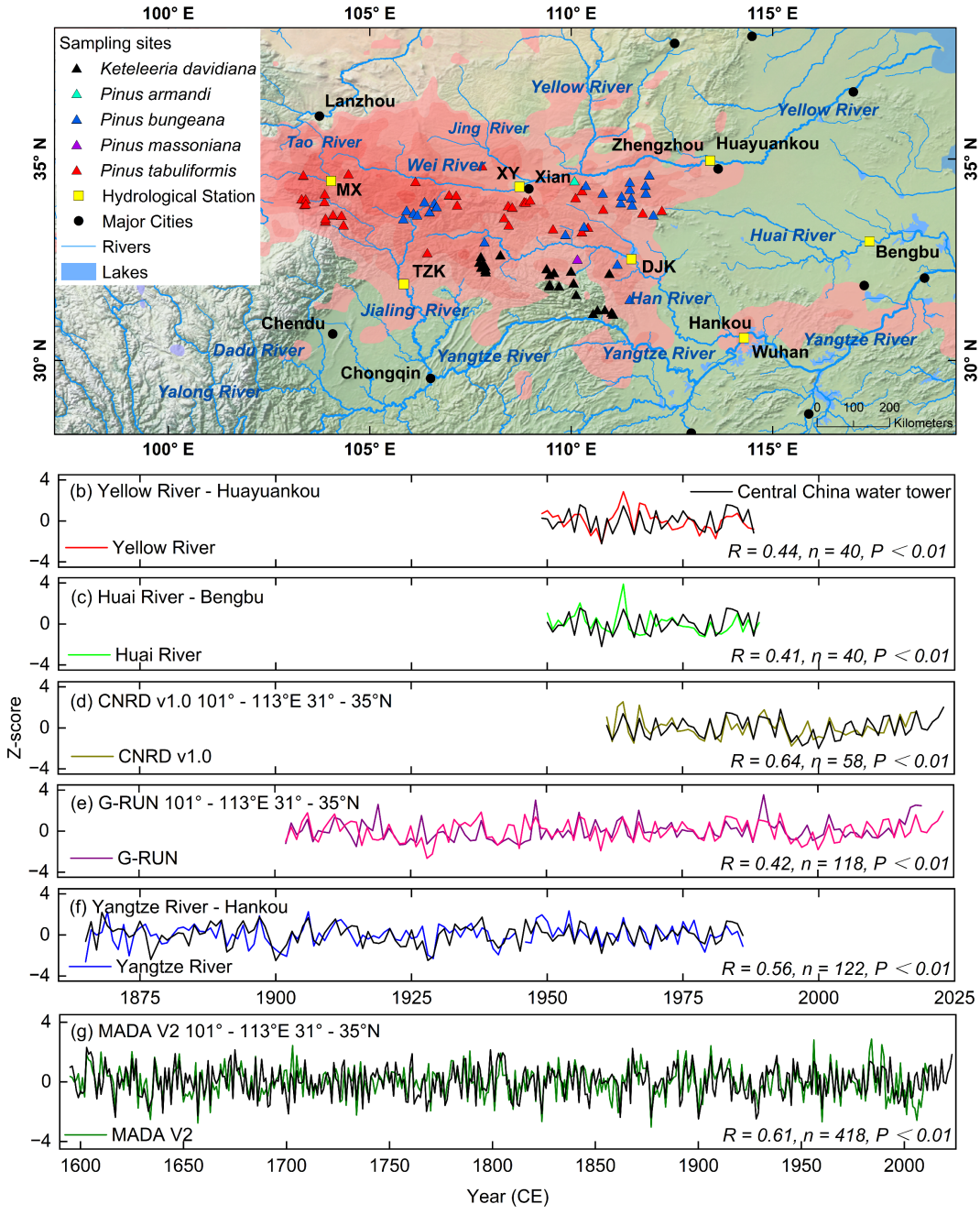

Figure S6. The water supply impact of the Central China water tower (CCWT) on surrounding basins and their shared connectivity. (a) Spatial distribution of the tree-

ring sampling network, major cities, hydrological stations, and rivers associated with the CCWT. (b) to (g) show the correlation results between observed runoff at hydrological control stations (including gridded hydroclimate data products, more information see Table S2 and Table S3) in the middle and lower reaches of the Yellow River, Huai River, and Yangtze River basins and the reconstructed runoff depth of the CCWT.

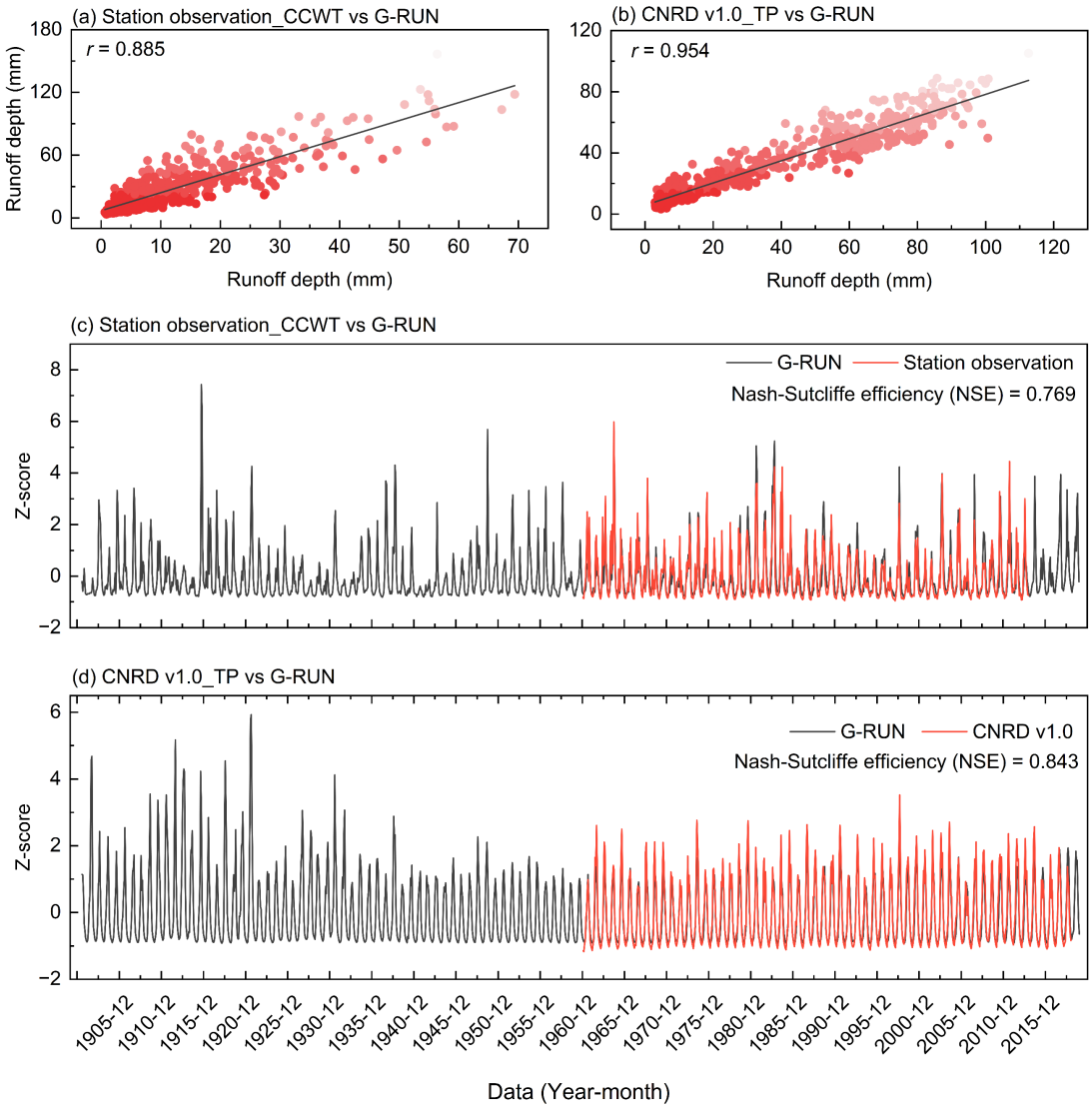

Figure S7 Comparison of G-RUN runoff data with station observations and regional gridded hydrological datasets. (a) and (b) show scatterplot regressions between G-RUN and CCWT hydrometric station observations, and between G-RUN and the regional

gridded dataset CNRD with TP, respectively, during overlapping periods. (c) and (d) display the corresponding time series comparisons. To enhance comparability, all series were standardized using Z-score transformation, as described in the Methods section of the manuscript.

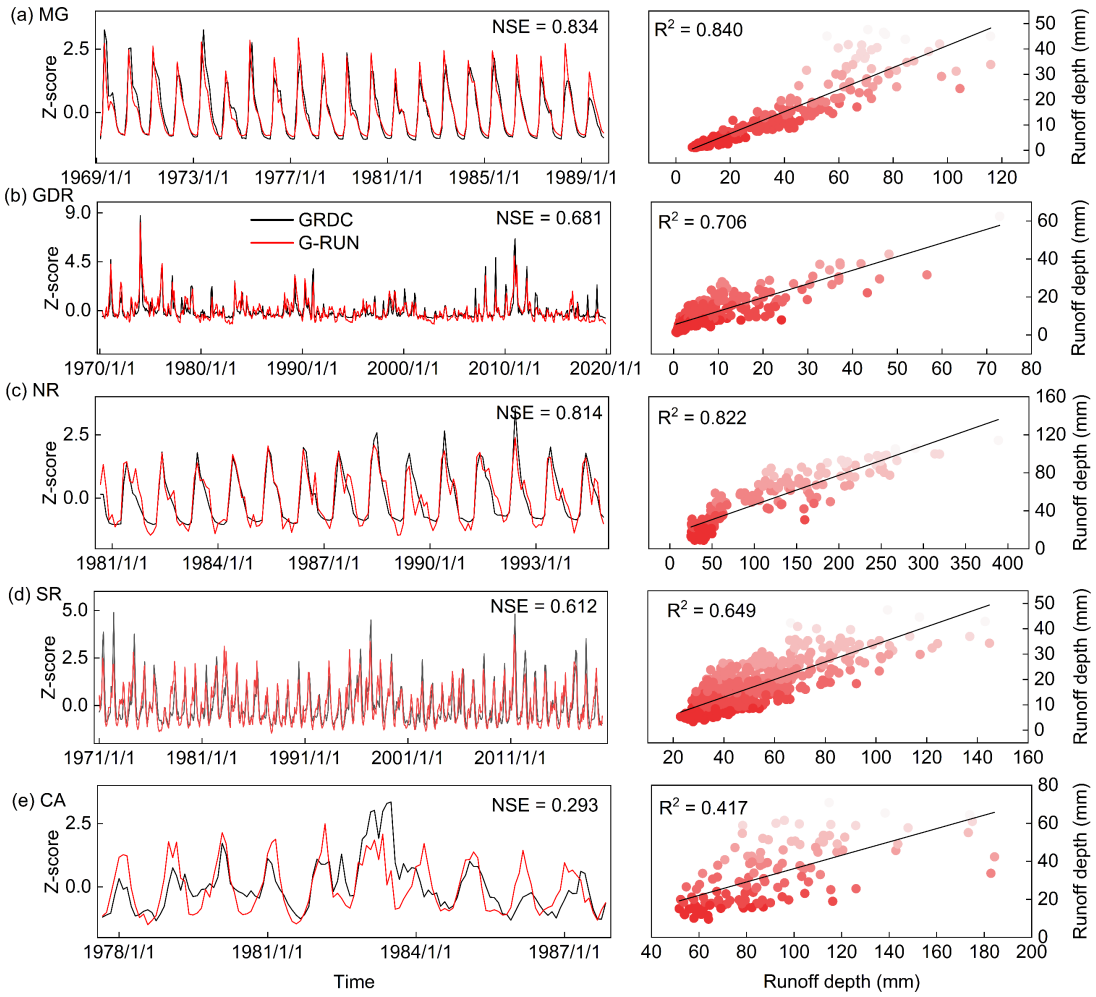

Figure S8 Comparison between observed station runoff depth and gridded G-RUN runoff depth. Panels (a) to (e) correspond to the MG, GDR, NR, SR, and CA water towers, respectively. The left subplots show the temporal variation of runoff during periods with continuous data coverage exceeding 60%. The right subplots display scatter plots and linear regressions between observed and G-RUN.

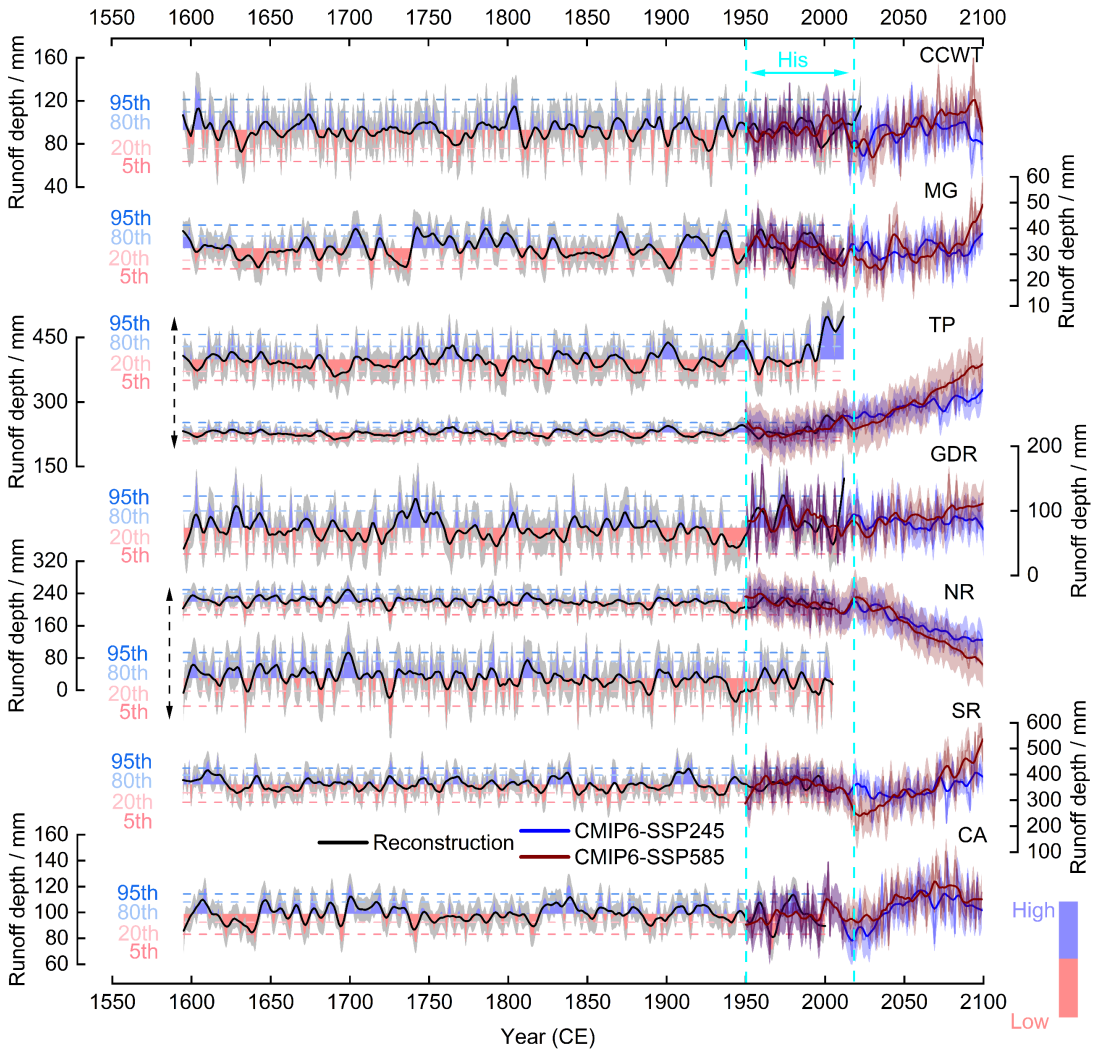

Figure S9. Reconstruction of runoff depth in the Pacific Rim water towers over the past four centuries compared with future projections from the CMIP6 multi-model ensemble mean. From top to bottom, they are the Central China water tower (CCWT), the Mongolian Plateau (MG), Tibetan Plateau (TP), Great Dividing Range (GDR), Northern Rockies (NR), Southern Rockies (SR), and Central Andes (CA). The magnitudes of TP and NR during the projection period exceed the highest levels of past historical reconstructions, so they are drawn twice, below and above them, respectively. Shaded lines represent the one-standard-deviation error of the reconstruction and projections. All reconstruction and projection results were subjected to an 11-year low-pass filter to capture low-frequency variations. Based on the mean, all reconstructed results were shaded above and below to distinguish high-runoff and low-runoff periods. Four

different colored dashed lines represent four distinct percentile thresholds of the reconstructed results.

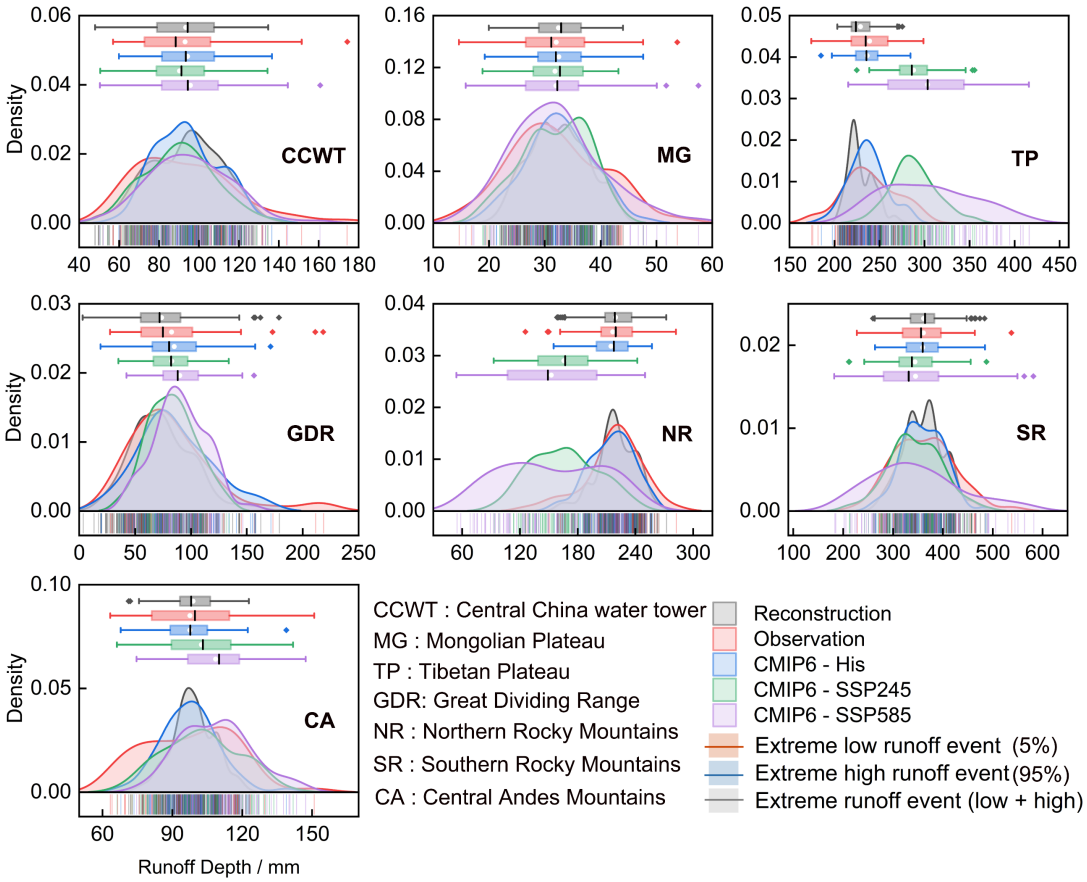

Figure S10. Distributions and box-plot characteristics of multi-year density for reconstructed, observed, and multi-model ensemble mean runoff depths for historical (His), low-emission scenario (SSP2-4.5), and high-emission scenario (SSP5-8.5) simulations and projections. The density distribution curves are smoothed using kernel density estimation and shaded downward. In the box plot, the black line represents the median, the white dot represents the mean, diamond symbols denote outliers, whiskers extend to 1.5 times the interquartile range, and the box spans the 25th to 75th percentiles.

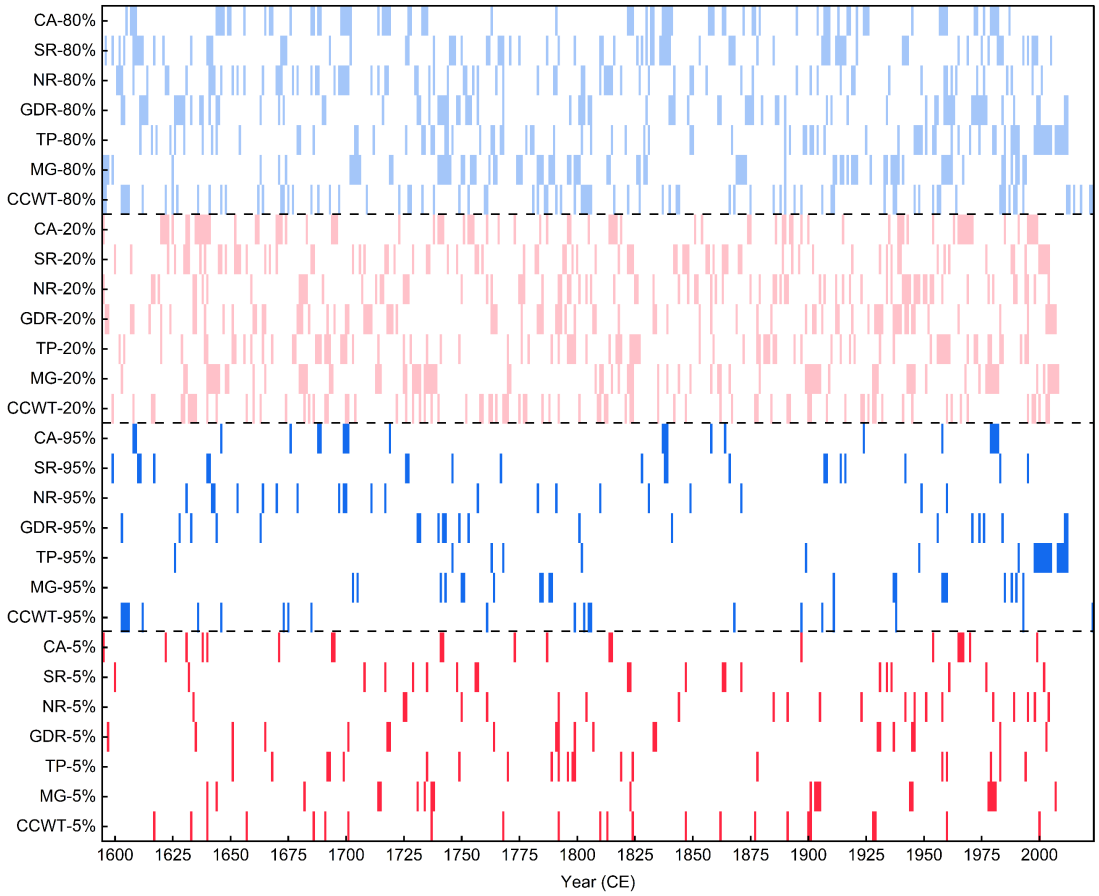

Figure S11. Hydrological drought and flood events identified from reconstructed runoff depth in the Pacific Rim water towers under different percentile thresholds. Red represents drought events, and blue represents flood events, with darker colors indicating more extreme events. From bottom to top, they are the Central China water tower (CCWT), the Mongolian Plateau (MG), Tibetan Plateau (TP), Great Dividing Range (GDR), Northern Rockies (NR), Southern Rockies (SR), and Central Andes (CA).

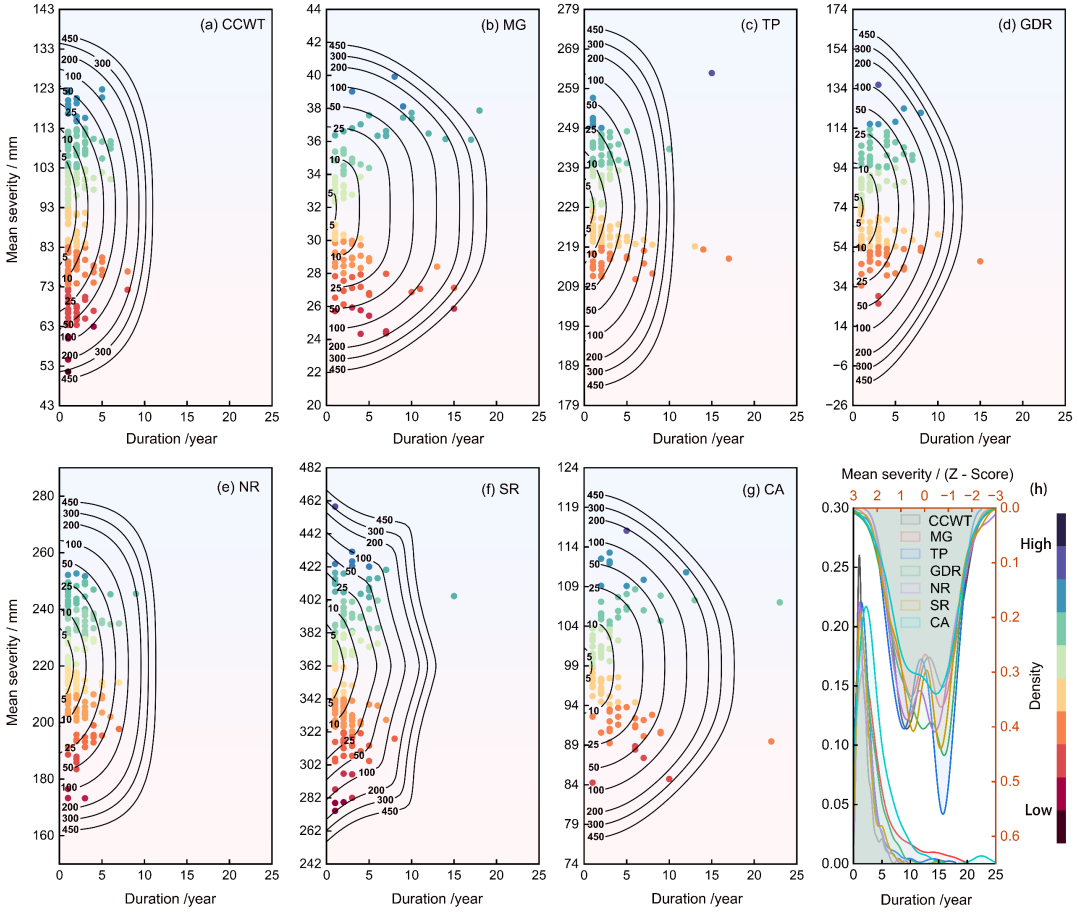

Figure S12. Analysis of high-runoff and low-runoff periods and estimation of recurrence intervals for runoff depth in the Pacific Rim water towers. Panels (a) to (g) display cumulative average severity and duration of high-runoff periods (blue solid circles) and low-runoff periods (red solid circles) of surface runoff depth for each region, including the Central China water tower (CCWT), Mongolian Plateau (MG), Tibetan Plateau (TP), Great Dividing Range (GDR), Northern Rockies (NR), Southern Rockies (SR), and Central Andes (CA), based on the continuous running of multi-year averages of reconstructed runoff depth. The contour lines for recurrence intervals (black) are derived from a copula function based on the joint probability of cumulative average severity and duration for both high-runoff and low-runoff periods. Solid circles are mapped above and below the mean of the reconstructed runoff depth to indicate severity. Panel (h) presents the density distributions of cumulative average severity (red axis) and duration (black axis) for high-runoff and low-runoff periods across the Pacific Rim water towers, with the cumulative average severity standardized using Z-scores for

comparison.

Table S1. Sampling sites and chronology development information

Number	Sites	Lon (E)	Lat (N)	Sampling Species	Tree/core	Integration Chronology	Length
1	QG	103.3	34.0	*Pinus tabuliformis*	29/56	QG	334
2	KES	103.3	34.6	*Pinus tabuliformis*	16/37	KES	409
3	KRQ	103.3	34.6	*Pinus tabuliformis*	17/26		
4	DLG	103.3	33.8	*Pinus tabuliformis*	25/43	DLG	352
5	SZY	103.4	34.0	*Pinus tabuliformis*	22/44	SZY	225
6	GJSY	103.4	33.8	*Pinus tabuliformis*	20/41	GJSY	359
7	MGY	103.8	33.9	*Pinus tabuliformis*	22/44	MGY	189
8	LZK	103.8	34.1	*Pinus tabuliformis*	25/49	LZK	191
9	RLY	103.9	33.4	*Pinus tabuliformis*	20/41	RLY	302
10	BLY	103.9	33.5	*Pinus tabuliformis*	28/56	BLY	185
11	JZY	104.0	33.6	*Pinus tabuliformis*	23/46	JZY	409
12	MNK	104.0	33.6	*Pinus tabuliformis*	24/49	MNK	382
13	ST	104.2	33.6	*Pinus tabuliformis*	20/41	ST	230
14	BYS	104.3	33.3	*Pinus tabuliformis*	23/54	BYS	123
15	BYY	104.3	33.3	*Pinus tabuliformis*			
16	JGS	104.4	34.6	*Pinus tabuliformis*	21/42	GQS	464
17	YSB	105.8	33.5	*Pinus bungeana*	7/13	YSB	153
18	DS	105.9	33.7	*Pinus bungeana*	37/69	DS	352
19	XSC	106.0	33.6	*Pinus bungeana*	23/46	XSC	252
20	SMS1	106.1	34.4	*Pinus tabuliformis*	20/53	SMS	407
21	SMS2	106.1	34.4	*Pinus tabuliformis*	13/29		
22	JYW	106.1	33.6	*Pinus bungeana*	21/42	JYW	222
23	LGX	106.3	33.9	*Pinus bungeana*	26/57	LGX	238

24	MBH	106.4	32.6	*Pinus tabuliformis*	20/36	MBH	200
25	YPS	106.4	33.6	*Pinus bungeana*	17/36	YPS	112
26	FYC	106.6	33.9	*Pinus bungeana*	45/91	LFGZ	402
27	LFGZ	106.6	33.8	*Pinus bungeana*			
28	JPC	106.6	33.8	*Pinus bungeana*			
29	LFG	106.6	33.8	*Pinus bungeana*			
30	HBS	106.6	33.8	*Pinus bungeana*			
31	SBY	106.9	34.1	*Pinus tabuliformis*	15/31	BJY	287
32	SBC	106.9	34.1	*Pinus tabuliformis*	1/4		
33	SHC	107.1	34.1	*Pinus tabuliformis*	2/6		
34	JPG	107.1	33.8	*Pinus tabuliformis*	3/6		
35	HQC	107.7	34.8	*Pinus tabuliformis*	3/7		
36	WZB	107.8	32.9	*Pinus bungeana*	21/53	WZB	326
37	HG	108.3	33.5	*Pinus tabuliformis*	36/71	HG	194
38	CZP	108.4	33.8	*Pinus tabuliformis*	40/80	CZP	324
39	SBS	108.4	33.3	*Pinus tabuliformis*	36/40	SBS	254
40	SBH	108.4	33.3	*Pinus tabuliformis*	16/33		
41	BLP	108.5	33.8	*Pinus tabuliformis*	21/42	BLP	89
42	GYS	108.8	33.9	*Pinus tabuliformis*	21/40	GYS	400
43	WHS	108.8	33.9	*Pinus tabuliformis*	24/50	WHS	293
44	NWT1	108.9	33.9	*Pinus tabuliformis*	21/42	NWT	228
45	NWT2	108.9	33.9	*Pinus tabuliformis*	27/59		
46	DZG	110.4	33.3	*Pinus tabuliformis*	2/4	SLY	246
47	YZC	109.5	33.2	*Pinus tabuliformis*	2/5		
48	MG	110.2	33.1	*Pinus tabuliformis*	2/4		
49	NSC	110.1	34.0	*Pinus tabuliformis*	2/6		
50	YJL	110.2	34.2	*Pinus tabuliformis*	19/39		
51	HSS	110.0	34.4	*Pinus armandi*	136/277	HSS	654
52	DLS	110.7	33.7	*Pinus tabuliformis*	24/43	DLS	83

53	WXS	110.3	34.3	*Pinus bungeana*	24/43	WXS	279
54	TQX	110.3	33.3	*Pinus bungeana*	2/8	HLB	301
55	MJG	110.7	34.1	*Pinus bungeana*	7/7		
56	HSY	111.2	33.9	*Pinus bungeana*	2/4		
57	WSB	111.2	33.9	*Pinus bungeana*	1/2		
58	MCB	111.2	34.0	*Pinus bungeana*	1/3		
59	YJF	111.9	34.6	*Pinus bungeana*	1/2		
60	BQC	111.8	34.3	*Pinus bungeana*	1/3		
61	DJF	111.4	34.2	*Pinus bungeana*	1/1		
62	LGB	111.4	34.4	*Pinus bungeana*	2/4		
63	XGC	111.4	34.0	*Pinus bungeana*	1/2		
64	ZYG	111.5	33.8	*Pinus bungeana*	1/2		
65	ZKC	111.5	33.8	*Pinus bungeana*	1/2		
66	ZWC	111.8	34.1	*Pinus bungeana*	1/2		
67	BSC	112.0	33.6	*Pinus bungeana*	1/3		
68	QLB	112.2	33.7	*Pinus tabuliformis*	20/40	QLB	255
69	LJL	111.7	33.6	*Pinus tabuliformis*	11/19	LJL	211
70	BYS	111.8	33.6	*Pinus tabuliformis*	15/27		
71	ZZS	110.1	32.5	*Pinus massoniana*	21/43	ZZS	209
72	BJS	111.1	32.3	*Pinus bungeana*	2/5	SYB	288
73	BKS	111.4	31.5	*Pinus bungeana*	4/8		
74	DZZ	109.8	33.1	*Pinus bungeana*	1/2		
75	FY	108.2	32.6	*Keteleeria davidiana*	2/3	TJYS	489
76	FXY	107.8	32.2	*Keteleeria davidiana*	2/4		
77	BLT	107.8	32.2	*Keteleeria davidiana*	1/2		
78	DYB	107.8	32.3	*Keteleeria davidiana*	1/2		
79	YJL	107.7	32.3	*Keteleeria davidiana*	1/2		
80	WJP	107.8	32.3	*Keteleeria davidiana*	1/3		
81	SJH	107.8	32.3	*Keteleeria davidiana*	1/2		

82	SLM	107.7	32.4	*Keteleeria davidiana*	2/4		
83	XFZ	107.8	32.4	*Keteleeria davidiana*	1/1		
84	BGC	107.7	32.5	*Keteleeria davidiana*	1/2		
85	DSC	109.4	31.8	*Keteleeria davidiana*	1/1		
86	SPC	109.4	31.8	*Keteleeria davidiana*	1/1		
87	HWC	109.4	32.1	*Keteleeria davidiana*	1/2		
88	HYC	109.5	32.1	*Keteleeria davidiana*	1/2		
89	LLZ	109.3	32.2	*Keteleeria davidiana*	1/2		
90	SSL	110.0	31.9	*Keteleeria davidiana*	7/26		
91	MJD	109.9	32.2	*Keteleeria davidiana*	3/6		
92	LTK	110.9	32.1	*Keteleeria davidiana*	3/6		
93	JDX	110.1	31.6	*Keteleeria davidiana*	3/6		
94	SST	110.0	31.9	*Keteleeria davidiana*	1/2		
95	FXS	109.6	31.8	*Keteleeria davidiana*	3/6		
96	GQS	110.5	31.1	*Keteleeria davidiana*	2/4		
97	YSS	110.6	31.2	*Keteleeria davidiana*	1/2		
98	HLD	110.8	31.2	*Keteleeria davidiana*	1/2		
99	DLP	111.0	31.2	*Keteleeria davidiana*	1/1		
100	SGP	111.0	31.1	*Keteleeria davidiana*	1/2		

Table S2. Chronology and drought atlas information

Name	Abbreviation	Lon (°)	Lat (°)	Period	Output indicators	Remark
Tree-ring chronology in the Qinling - Daba Mountains	CCWT	103.3–112.2 E	31.1–34.8 N	1359–2023	TRW	CCWT
Monsoon Asia Drought Atlas version 2	MADA v2	82–124 E	47–53 N	0–2012	scPDSI	MG
		90–99 E	28–37 N	0–2012	scPDSI	TP
Eastern Australia and New Zealand Drought Atlas	ANZDA	144–154 E	39–14 S	1500–2012	scPDSI	GDR
North American Drought Atlas	NADA	145–122 W	54–66 N	0–2005	scPDSI	NR
		124–103 W	32 – 54 N	0–2005	scPDSI	SR
South American Drought Atlas	SADA	70–50.25 W	12.25–30 S	1400–2000	scPDSI	CA

Notes: The abbreviations are the Central China water tower (CCWT), the Mongolian Plateau (MG), Tibetan Plateau (TP), Great Dividing Range (GDR), Northern Rockies (NR), Southern Rockies (SR), and Central Andes (CA).

Table S3. Hydrological data information

Name	Abbreviation	Lon (°)	Lat (°)	Period	Remark
Tao River	MX / Minxian	104.0 E	34.4 N	1961–2013	CCWT
Wei River	XY / Xianyang	108.7 E	34.3 N		
Jialing River	TZK / Tingzhikou	105.8 E	31.8 N		
Han River	DJK / Danjiangkou	111.5 E	32.5 N		
The China Natural Runoff Dataset version 1.0	CNRD v1.0	90–99 E	28–37 N	1961–2018	TP
Global RUNoff ENSEMBLE	G-RUN ENSEMBLE	82–124 E	47–53 N	1901–2019	MG
		144–154 E	39–14 S	1901–2019	GDR
		145–122 W	54–66 N	1901–2019	NR
		124–103 W	32–54 N	1901–2019	SR
		70–50.25 W	12.25–30 S	1901–2019	CA

Notes: The abbreviations are the Central China water tower (CCWT), the Mongolian Plateau (MG), Tibetan Plateau (TP), Great Dividing Range (GDR), Northern Rockies (NR), Southern Rockies (SR), and Central Andes (CA).

Table S4. Best key parameters for each model

Model	CCWT	MG	TP
Linear Regression	Cross-validated MSE: 0.615	Cross-validated MSE: 0.740	Cross-validated MSE: 0.530
Ridge Regression	Alpha: 10.0	Alpha: 10.0	Alpha: 10.0
Lasso Regression	Alpha: 0.1	Alpha: 0.1	Alpha: 0.1
ElasticNet Regression	Alpha: 0.1 L1 ratio: 0.1	Alpha: 0.1 L1 ratio: 0.1	Alpha: 0.1 L1 ratio: 0.1
Huber Regression	Epsilon: 1.1	Epsilon: 1.1	Epsilon: 1.5
Random Forest	Max depth: 2 Min samples split: 20 N estimators: 50	Max depth: 3 Min samples split: 20 N estimators: 50	Max depth: 4 Min samples split: 20 N estimators: 50
Gradient Boosting	Learning rate: 0.01 Max depth: 2 N estimators: 100	Learning rate: 0.01 Max depth': 2 N estimators: 200	Learning rate: 0.01 Max depth: 2 N estimators: 200
Xtreme Gradient Boosting	Learning rate: 0.01 Max depth: 2 N estimators: 100	Learning rate: 0.01 Max depth: 2 N estimators: 200	Learning rate: 0.01 Max depth: 2 N estimators: 200

Notes: The abbreviations are the Central China water tower (CCWT), the Mongolian Plateau (MG), Tibetan Plateau (TP), Great Dividing Range (GDR), Northern Rockies (NR), Southern Rockies (SR), and Central Andes (CA).

Table S5. Best key parameters for each model

Model	GDR	NR	SR	CA
Linear Regression	Cross-validated MSE: 0.294	Cross-validated MSE: 0.495	Cross-validated MSE: 0.604	Cross-validated MSE: 0.677
Ridge Regression	Alpha: 1.0	Alpha: 10.0	Alpha: 10.0	Alpha: 10.0
Lasso Regression	Alpha: 0.1	Alpha: 0.1	Alpha: 0.01	Alpha: 0.1
ElasticNet Regression	Alpha: 0.1 L1 ratio: 0.1	Alpha: 0.1 L1 ratio: 0.9	Alpha: 0.1 L1 ratio: 0.1	Alpha: 0.1 L1 ratio: 0.1
Huber Regression	Epsilon: 1.35	Epsilon: 1.35	Epsilon: 1.5	Epsilon: 1.1
Random Forest	Max depth: 3 Min samples split: 10 N estimators: 50	Max depth: 4 Min samples split: 20 N estimators: 50	Max depth: 3 Min samples split: 10 N estimators: 50	Max depth: 2 Min samples split: 20 N estimators: 50
Gradient Boosting	Learning rate: 0.01 Max depth: 2 N estimators: 200	Learning rate: 0.01 Max depth: 2 N estimators: 200	Learning rate: 0.05 Max depth: 2 N estimators: 50	Learning rate: 0.01 Max depth: 2 N estimators: 100
Xtreme Gradient Boosting	Learning rate: 0.05 Max depth: 2 N estimators: 50	Learning rate: 0.01 Max depth: 2 N estimators: 200	Learning rate: 0.05 Max depth: 2 N estimators: 50	Learning rate: 0.01 Max depth: 2 N estimators: 200

Notes: The abbreviations are the Central China water tower (CCWT), the Mongolian Plateau (MG), Tibetan Plateau (TP), Great Dividing Range (GDR), Northern Rockies (NR), Southern Rockies (SR), and Central Andes (CA).

Table S6. Statistical characteristics of the reconstruction models (Central China water tower)

Model	R2	RE1	PMT	RE2	ST	NSEC	RMSD	KGE
Linear Regression	48.4%	84.1%	7.84	0.44	46+/7-	0.48	17.9	0.60
Ridge Regression	48.4%	82.9%	7.84	0.44	46+/7-	0.47	17.9	0.52
Lasso Regression	48.4%	83.1%	7.84	0.44	46+/7-	0.48	17.9	0.53
ElasticNet Regression	48.4%	83.4%	7.84	0.44	46+/7-	0.48	17.9	0.55
Huber Regression	48.4%	-373.1%	7.84	0.44	46+/7-	0.46	18.3	0.59
Random Forest	54.4%	96%	8.67	0.50	44+/9-	0.54	16.8	0.60
Gradient Boosting	58.8%	67.6%	6.67	0.55	47+/6-	0.50	17.5	0.43
Xtreme Gradient Boosting	57.0%	55.5%	7.30	0.53	41+/12-	0.48	17.8	0.41
Ensemble mean	52.0%	22.4%	8.31	0.48	46+/7-	0.51	17.4	0.53

Notes: R2: variance explained, RE1: relative bias in percent, PMT: product mean test, RE2: reduction of error, ST: sign test, NSEC: Nash Sutcliffe model Efficiency coefficient, RMSD: Root Mean Square Deviation, KGE: Kling-Gupta efficiency.

Table S7. Statistical characteristics of the reconstruction models (Mongolian Plateau)

Model	R2	RE1	PMT	RE2	ST	NSEC	RMSD	KGE
Linear Regression	51.9%	2.8%	7.06	0.47	42+/10-	0.83	5.7	0.64
Ridge Regression	51.9%	2.9%	7.06	0.47	42+/10-	0.83	5.7	0.55
Lasso Regression	51.9%	2.8%	7.06	0.47	42+/10-	0.83	5.7	0.57
ElasticNet Regression	51.9%	2.8%	7.06	0.47	42+/10-	0.83	5.7	0.59
Huber Regression	51.9%	-79.4%	7.06	0.47	42+/10-	0.83	5.8	0.62
Random Forest	56.5%	-7.1%	8.96	0.52	43+/9-	0.85	5.4	0.63
Gradient Boosting	64.0%	-2.1%	7.27	0.61	43+/9-	0.87	5.0	0.62
Xtreme Gradient Boosting	62.6%	-4.4%	7.63	0.51	42+/10-	0.86	5.1	0.60
Ensemble mean	56.6%	-10.2%	7.52	0.53	43+/9-	0.85	5.4	0.61

Notes: R2: variance explained, RE1: relative bias in percent, PMT: product mean test, RE2: reduction of error, ST: sign test, NSEC: Nash Sutcliffe model Efficiency coefficient, RMSD: Root Mean Square Deviation, KGE: Kling-Gupta efficiency.

Table S8. Statistical characteristics of the reconstruction models (Tibetan Plateau)

Model	R2	RE1	PMT	RE2	ST	NSEC	RMSD	KGE
Linear Regression	50.4%	-44.6%	8.06	0.46	42+/10-	0.62	21.0	0.63
Ridge Regression	50.4%	-40.9%	8.06	0.46	42+/10-	0.62	20.9	0.55
Lasso Regression	50.4%	-41.5%	8.06	0.46	42+/10-	0.62	20.9	0.56
ElasticNet Regression	50.4%	-42.3%	8.06	0.46	42+/10-	0.62	20.9	0.58
Huber Regression	50.4%	58%	8.06	0.46	42+/10-	0.62	20.9	0.62
Random Forest	60.7%	-91.6%	10.33	0.57	43+/9-	0.70	18.6	0.68
Gradient Boosting	70.5%	-32.2%	8.66	0.67	44+/8-	0.76	16.5	0.67
Xtreme Gradient Boosting	67.9%	-26.1%	8.84	0.65	44+/8-	0.74	17.2	0.65
Ensemble mean	58.2%	-32.6%	8.81	0.54	42+/10-	0.68	19.2	0.62

Notes: R2: variance explained, RE1: relative bias in percent, PMT: product mean test, RE2: reduction of error, ST: sign test, NSEC: Nash Sutcliffe model Efficiency coefficient, RMSD: Root Mean Square Deviation, KGE: Kling-Gupta efficiency.

Table S9. Statistical characteristics of the reconstruction models (Great Dividing Range)

Model	R2	RE1	PMT	RE2	ST	NSEC	RMSD	KGE
Linear Regression	75.8%	151.6%	4.31	0.72	46+/5-	0.83	19.6	0.84
Ridge Regression	75.8%	152.1%	4.31	0.72	46+/5-	0.83	19.5	0.83
Lasso Regression	75.8%	154.7%	4.31	0.72	46+/5-	0.83	19.5	0.78
ElasticNet Regression	75.8%	154.4%	4.31	0.72	46+/5-	0.83	19.5	0.79
Huber Regression	75.8%	-79.4%	4.31	0.72	46+/5-	0.83	19.6	0.76
Random Forest	86.2%	-36.7%	3.83	0.83	47+/4-	0.90	14.7	0.88
Gradient Boosting	88.3%	51.9%	3.48	0.85	48+/3-	0.91	14.4	0.80
Xtreme Gradient Boosting	87.9%	14.2%	3.55	0.85	48+/3-	0.91	14.3	0.82
Ensemble mean	82.3%	70.4%	4.04	0.79	46+/5-	0.87	16.8	0.81

Notes: R2: variance explained, RE1: relative bias in percent, PMT: product mean test, RE2: reduction of error, ST: sign test, NSEC: Nash Sutcliffe model Efficiency coefficient, RMSD: Root Mean Square Deviation, KGE: Kling-Gupta efficiency.

Table S10. Statistical characteristics of the reconstruction models (Northern Rockies)

Model	R2	RE1	PMT	RE2	ST	NSEC	RMSD	KGE
Linear Regression	56.9%	-8.4%	5.05	0.52	38+/13-	0.66	19.9	0.69
Ridge Regression	56.9%	-16.4%	5.05	0.52	38+/13-	0.66	19.9	0.61
Lasso Regression	56.9%	-14.6%	5.05	0.52	38+/13-	0.67	19.8	0.63
ElasticNet Regression	56.9%	-14.3%	5.05	0.52	38+/13-	0.67	19.8	0.64
Huber Regression	56.9%	-109.4%	5.05	0.52	38+/13-	0.66	19.9	0.69
Random Forest	70.9%	11.8%	4.16	0.68	40+/11-	0.77	16.3	0.75
Gradient Boosting	76.1%	36.9%	3.75	0.74	40+/11-	0.80	15.3	0.71
Xtreme Gradient Boosting	74.2%	57.8%	3.77	0.72	38+/13-	0.78	15.9	0.68
Ensemble mean	65.3%	-7.1%	4.60	0.61	38+/13-	0.73	17.9	0.68

Notes: R2: variance explained, RE1: relative bias in percent, PMT: product mean test, RE2: reduction of error, ST: sign test, NSEC: Nash Sutcliffe model Efficiency coefficient, RMSD: Root Mean Square Deviation, KGE: Kling-Gupta efficiency.

Table S11. Statistical characteristics of the reconstruction models (Southern Rockies)

Model	R2	RE1	PMT	RE2	ST	NSEC	RMSD	KGE
Linear Regression	49.9%	7.1%	6.55	0.45	39+/12-	0.49	42.9	0.62
Ridge Regression	49.9%	15.8%	6.55	0.45	39+/12-	0.49	42.8	0.55
Lasso Regression	49.9%	7.8%	6.55	0.45	39+/12-	0.49	42.9	0.62
ElasticNet Regression	49.9%	12.3%	6.55	0.45	39+/12-	0.49	42.7	0.58
Huber Regression	49.9%	-150.6%	6.55	0.45	39+/12-	0.49	42.9	0.61
Random Forest	62.6%	-209.9%	5.94	0.59	40+/11-	0.62	37.1	0.66
Gradient Boosting	68.2%	-85%	4.70	0.66	41+/10-	0.67	34.7	0.66
Xtreme Gradient Boosting	64.5%	-116.4%	5.07	0.62	41+/10-	0.63	36.6	0.63
Ensemble mean	56.7%	-64.9%	6.05	0.52	39+/12-	0.56	39.8	0.62

Notes: R2: variance explained, RE1: relative bias in percent, PMT: product mean test, RE2: reduction of error, ST: sign test, NSEC: Nash Sutcliffe model Efficiency coefficient, RMSD: Root Mean Square Deviation, KGE: Kling-Gupta efficiency.

Table S12. Statistical characteristics of the reconstruction models (Central Andes)

Model	R2	RE1	PMT	RE2	ST	NSEC	RMSD	KGE
Linear Regression	42.0%	22.9%	6.70	0.37	36+/15-	0.41	14.9	0.54
Ridge Regression	42.0%	21.3%	6.70	0.37	36+/15-	0.41	14.9	0.46
Lasso Regression	42.0%	21.5%	6.70	0.37	36+/15-	0.41	14.9	0.47
ElasticNet Regression	42.0%	22%	6.70	0.37	36+/15-	0.42	14.8	0.49
Huber Regression	42.0%	-35.5%	6.70	0.37	36+/15-	0.41	14.9	0.54
Random Forest	45.8%	33.8%	7.63	0.41	36+/15-	0.45	14.4	0.49
Gradient Boosting	50.5%	11.6%	6.03	0.46	33+/18-	0.43	14.6	0.37
Xtreme Gradient Boosting	52.3%	12.8%	6.14	0.48	37+/14-	0.50	13.7	0.49
Ensemble mean	45.2%	13.8%	6.66	0.40	36+/15-	0.44	14.5	0.49

Notes: R2: variance explained, RE1: relative bias in percent, PMT: product mean test, RE2: reduction of error, ST: sign test, NSEC: Nash Sutcliffe model Efficiency coefficient, RMSD: Root Mean Square Deviation, KGE: Kling-Gupta efficiency.

Table S13. Information about the 24 GCM models provided by CMIP6

Number	Model	Full name	Source	Resolution
1	ACCESS-CM2	Australian Community Climate and Earth-System Simulator - Coupled Model version 2	Australia	250 km
2	ACCESS-ESM1-5	Australian Community Climate and Earth-System Simulator Earth System Model version 1.5	Australia	250 km
3	BCC-CSM2-MR	Beijing Climate Center Climate System Model version 2 - Medium Resolution	China	100 km
4	CanESM5	Canadian Earth System Model version 5	Canada	100 km
5	CAS-ESM2-0	Chinese Academy of Sciences Earth System Model version 2	China	100 km
6	CESM2-WACCM	Community Earth System Model version 2 - Whole Atmosphere Community Climate Model	America	100 km
7	CMCC-CM2-SR5	CMCC Climate Model version 2 - Standard Resolution 5	Italy	100 km
8	CMCC-ESM2	CMCC Earth System Model version 2	Italy	100 km
9	EC-Earth3	European Consortium Earth System Model, version 3	Europe	80 km
10	EC-Earth3-Veg	European Consortium Earth System Model, version 3 - Vegetation	Europe	80 km
11	EC-Earth3-Veg-LR	European Consortium Earth System Model, version 3 - Vegetation - Low Resolution	Europe	100 km

12	FGOALSf3-L	Flexible Global Ocean-Atmosphere-Land System model	China	100 km
13	FGOALS-g3	Flexible Global Ocean-Atmosphere-Land System model, Grid-point version 3	China	100 km
14	GFDL-ESM4	Geophysical Fluid Dynamics Laboratory Earth System Model version 4	America	100 km
15	INM-CM4-8	Institute of Numerical Mathematics Climate Model version 4.8	Russia	150 km
16	INM-CM5-0	Institute of Numerical Mathematics Climate Model version 5.0	Russia	150 km
17	IPSL-CM6A-LR	Institut Pierre-Simon Laplace Climate Model version 6 - Low Resolution	Europe	150 km
18	KACE-1-0-G	Korea Advanced Climate Ecosystem Model version 1.0-G	Korea	100 km
19	MCM-UA-1-0	Malmö University Climate Model version UA 1.0	Sweden	100 km
20	MIROC6	Model for Interdisciplinary Research on Climate version 6	Japan	140 km
21	MPI-ESM1-2-HR	Max Planck Institute Earth System Model version 1.2 - High Resolution	Germany	25 km
22	MPI-ESM1-2-LR	Max Planck Institute Earth System Model version 1.2 - Low Resolution	Germany	100 km
23	MRI-ESM2-0	Meteorological Research Institute Earth System Model version 2.0	Japan	100 km
24	NorESM2-LM	Norwegian Earth System Model version 2	Norway	100 km

Table S14. Frequency of hydrological events projected by CMIP6 models for each Pacific Rim water tower

Name	Scenarios	5%	20%	80%	95%
CCWT	Threshold line	63.62 mm	75.79 mm	109.68 mm	121.18 mm
	SSP2-4.5	4	20	12	4
	SSP5-8.5	3	13	20	8
MG	Threshold line	24.33 mm	27.69 mm	37.09 mm	41.33 mm
	SSP2-4.5	13	19	20	3
	SSP5-8.5	13	25	18	10
TP	Threshold line	209.47 mm	217.72 mm	240.91 mm	252.06 mm
	SSP2-45	0	0	82	78
	SSP5-85	0	0	78	71
GDR	Threshold line	33.10 mm	51.84 mm	99.86 mm	122.92 mm
	SSP2-45	0	5	16	3
	SSP5-85	0	5	28	7
NR	Threshold line	187.10 mm	204.53 mm	239.09 mm	249.21 mm
	SSP2-45	62	70	1	0
	SSP5-85	58	67	2	1
SR	Threshold line	292.65 mm	328.98 mm	397.35 mm	423.98 mm
	SSP2-45	14	34	13	5
	SSP5-85	26	41	21	16
CA	Threshold line	83.26 mm	92.40 mm	108.06 mm	114.36 mm
	SSP2-45	13	23	29	22
	SSP5-85	3	13	44	29

Notes: Events are identified using percentile-based thresholds derived from the reconstructed runoff depth series (Threshold line / mm). The abbreviations are the

Central China water tower (CCWT), the Mongolian Plateau (MG), Tibetan Plateau (TP), Great Dividing Range (GDR), Northern Rockies (NR), Southern Rockies (SR), and Central Andes (CA).

Table S15. Change points in reconstructed and projected runoff depth variations of the Pacific Rim water towers ($P < 0.05$)

Name	Reconstruction	SSP2-4.5	SSP5-8.5
CCWT	\	\	2014, 2037, 2058
MG	1649, 1712, 1739, 1806, 1910, 1941	1999	1999, 2040, 2080
TP	1887, 1907, 1935, 1955, 1987	2007, 2043, 2079	2006, 2040, 2065
GDR	1729, 1758, 1953	\	2075
NR	1937	2000, 2038, 2064	1996, 2027, 2052, 2078
SR	\	1999, 2070	2016, 2040, 2070
CA	1641, 1697, 1736, 1821, 1841	2010, 2040	2036

Note: The abbreviations are the Central China water tower (CCWT), the Mongolian Plateau (MG), Tibetan Plateau (TP), Great Dividing Range (GDR), Northern Rockies (NR), Southern Rockies (SR), and Central Andes (CA).